Macromolecules

Article

Cite This: Macromolecules 2018, 51, 3932−3940

Alternating Ring-Opening Metathesis Polymerization (AROMP) of Hydrophobic and Hydrophilic Monomers Provides Oligomers with Side-Chain Sequence Control

Guofang Li and Nicole S. Sampson*

Department of Chemistry, Stony Brook University, Stony Brook, New York 11794-3400, United States

Supporting Information

ABSTRACT: We report the formation of oligomers with side-chain sequence control using ruthenium-catalyzed alternating ring-opening metathesis polymerization (AROMP). These oligomers are prepared through sequential, stoichiometric addition of bicyclo[4.2.0]oct-1(8)-ene-8-carboxamide (monomer A) at 85 °C and cyclohexene (monomer B) at 45 °C to generate sequences up to 24 monomeric units composed of (**A**-*alt*-**B**)$_n$ and (**A**′-*alt*-**B**)$_n$ microblocks, where n ranges from 1 to 6. Herein, monomer **A** has an alkyl side chain, and monomer **A**′ has a glycine methyl ester side chain. Increasing microblock size from one to six results in an increasing water contact angle on spin-coated thin films, despite the constant ratio of hydrophilic and hydrophobic moieties. However, a disproportionately high contact angle was observed when n equals 2. Thus, the unique all-carbon backbone formed in the AROMP of bicyclo[4.2.0]oct-1(8)-ene-8-carboxamides and cyclohexene provides a platform for the nontemplated preparation of materials with specific sequences of side chains.

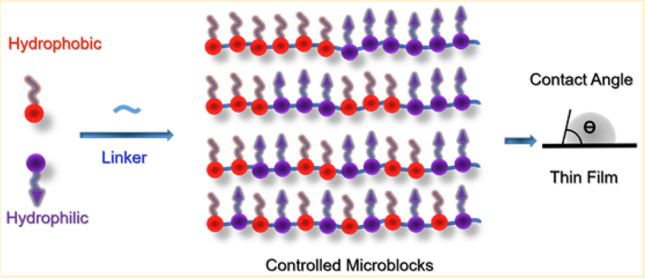

INTRODUCTION

Copolymers with well-controlled microstructure display superior morphology and enhanced properties, such as spatial organization, folding, and self-assembly.[1] Sequence control is essential for applications of synthetic polymers as advanced materials, where the position of monomers impacts functionality and performance.[2] Syntheses of precision polymers that rely on the specificity of enzymes and the fidelity of templates have been very successful. However, nontemplated polymer synthesis is still highly limited in terms of functional complexity, backbone structure, and sequence.[3]

Two synthetic methods based on step-growth or chain-growth reactions have been widely applied to obtain nontemplated sequence control. Step-growth synthesis is conducted via iterative addition of AB-type bifunctional monomers to obtain high yield and high scalability.[4] However, with terminal activation or deprotection involved in each step, reaction efficiency is limited by multiple purification steps and monomer reactivity. Recently, monomers with orthogonal reaction sites have been developed for rapid assembly of sequence-defined polymers on a liquid support.[5] Chain-growth synthesis include atom transfer radical polymerization (ATRP),[6] reversible addition−fragmentation chain transfer polymerization (RAFT),[7] and nitroxide-mediated polymerization (NMP).[8] Monomer pairs which favor cross-reactivity over homopolymerization are applied to control the placement of monomer units in the polymer chain. Although appreciable progress has been made, application of these chemistries relies on kinetically favored cross-propagation, applying either time-controlled[8] or temperature-controlled[9] monomer incorporation.

Ring-opening metathesis polymerization (ROMP) has been recently introduced in the chain-growth, precision polymer arena. Polymers with repeating sequences have been synthesized via incorporation of multiple functional groups on cyclooctenes[10] or macrocycles[11] followed by ROMP. Early implementation of ROMP employed large excesses of monomers[12,13] to generate alternating polymers or statistical equilibration postpolymerization.[14] Various alternating ring-opening metathesis polymerization (AROMP) systems based on monomer or catalyst design have been adapted to obtain sequence control.[15−18]

AROMP based on 1-substituted cyclobutenes and cyclohexene yields copolymers with a strictly alternating monomer distribution.[19,20] Neither monomer forms homopolymer under ROMP conditions, eliminating the need for use of excess monomer to ensure alternation. Several cyclobutene systems have been developed.[20−22] Bicyclo[4.2.0]oct-1(8)-ene-8-carboxamides, **1**, when used in combination with cyclohexene, **2**, react rapidly to provide long, linear copolymers,[21] and the carboxamide monomers are readily prepared.[23] The reaction characteristics suggested that AROMP of bicyclo[4.2.0]oct-1(8)-ene-8-carboxamides with cyclohexene might provide an avenue to prepare copolymers with monomer sequence control.

Received: March 15, 2018
Revised: May 5, 2018
Published: May 15, 2018

DOI: 10.1021/acs.macromol.8b00562
Macromolecules 2018, 51, 3932−3940

Scheme 1. Oligomers of Controlled Sequences Are Prepared by Sequential Monomer Addition: (A) General Synthetic Approach To Prepare Oligomers with Controlled Side-Chain Sequence; (B) Cartoon Illustration of Oligomers Prepared.[a]

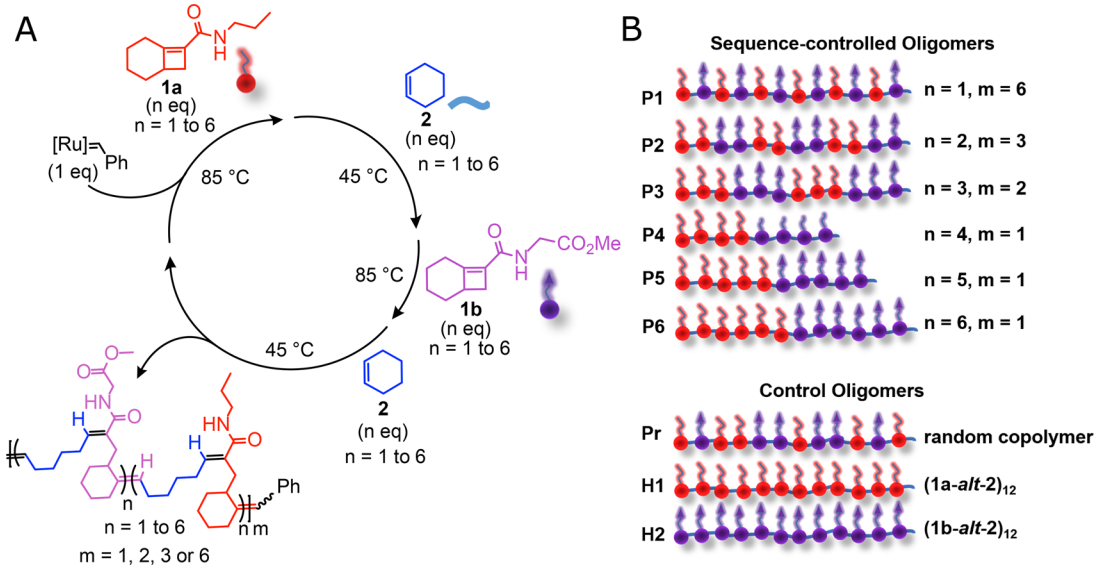

[a]Sequence-controlled oligomers are synthesized iteratively as outlined in (A). Control oligomers are synthesized by AROMP of the indicated mixture of monomers in a single cycle of polymerization.

Herein, we report development of an AROMP-based method for stepwise incorporation of one to six bicyclo[4.2.0]oct-1(8)-ene-8-carboxamide monomers into a growing, alternating oligomeric chain via sequential, stoichiometric monomer addition (Scheme 1). Essentially, cyclohexene is utilized as a linker between carboxamides, which can contain different side chains. Sequence-controlled multiblock oligomers were successfully synthesized with a constant ratio of hydrophilic and hydrophobic side chains presented in different alternating sequences. We observed that microblock size dictated surface properties of thin films. Thus, the AROMP-based strategy provides an all-carbon backbone platform for the preparation of materials with well-controlled side-chain sequences that determine material properties.

EXPERIMENTAL SECTION

General Materials and Methods. All metathesis reactions were performed under an N_2 atmosphere. Solvents used for ring-opening reactions and deuterated solvents used for NMR spectroscopy were degassed and filtered through basic alumina before use. Catalyst $Cl_2(H_2IMes)(PCy_3)Ru{=}CHPh$ and poly(styrene) standards were purchased from Aldrich. Monomer **1** was prepared as reported.[21,23] Cyclohexene **2** was distilled from CaH_2 prior to use. The synthesis of catalyst $(3\text{-Br-Pyr})_2Cl_2(H_2IMes)Ru{=}CHPh$, **3**, was performed according to the procedure of Love et al.[24]

The mass spectrometric measurements were performed on a Micromass Premier quadrupole time-of-flight (Q-Tof) instrument (Waters, Manchester) equipped with an ESI ion source containing a stainless-steel metal spray capillary (127 μm inner diameter, 229 μm outer diameter, 181 mm length). A sample or aliquot of reaction mixture was diluted in CH_2Cl_2 to a final concentration of 50 μg/mL and utilized for measurement. A capillary voltage of 3.5 kV, source and desolvation temperatures of 50 °C, and a cone voltage of 20 V were utilized as standard ESI operating conditions. Collision-induced dissociation (CID, collision gas Ar with flow rate at 0.2 mL/min) was performed in the collision cell region; the collision energy was set to 2−30 eV for different ion species.

Mallinckrodt silica gel 60 (230−400 mesh) was used for column chromatography. Analytical thin layer chromatography (TLC) was performed on precoated silica gel plates (60F254), flash chromatography on silica gel-60 (230−400 mesh), and Combi-Flash chromatography on RediSep normal phase silica columns (silica gel-60, 230−400 mesh). Bruker Nanobay 400, Avance III 500, and Avance III 700 NMR instruments were used for analysis. ^{1}H NMR and ^{13}C NMR spectra were collected under an N_2 atmosphere in CD_2Cl_2. ^{1}H NMR spectra are reported as chemical shift in parts per million (multiplicity, coupling constant in hertz, integration). ^{1}H NMR data are assumed to be first order. Molecular weights and molar mass dispersities were measured on a Phenogel 5 μm 10E4A LC column (300 × 7.8 mm, 5 μm, linear mixed bed, 0−500K MW range, Phenomenex) with a chromatography system constructed from a Shimadzu pump coupled to a differential refractometer and a Shimadzu UV detector. THF served as the eluent with a flow rate of 0.7 mL/min at 30 °C. All GPC chromatograms were calibrated with narrowly dispersed poly(styrene) standards from Aldrich or Agilent. The number- and weight-average molecular weights were calculated based on the refractive index and UV absorption signal.

Procedure for Monitoring the Rate of AROMP Reactions. Rates of alternating ring-opening metathesis polymerization for selected monomers **1** were measured under an N_2 atmosphere in a capped NMR tube, and ^{1}H NMR spectra were acquired at 35 °C. Amide monomer **1** (10 μmol, 10 equiv) was dissolved in 300 μL of $CDCl_3$ and mixed with 200 μL of fresh catalyst **3** (1 μmol, 1 equiv). Completion of initiation was measured as the disappearance of the ruthenium alkylidene resonance at 19.1 ppm in the ^{1}H NMR spectrum. Cyclohexene **2** (20 μmol, 20 equiv) was then added, and the reaction was heated at 35 °C. Reaction progress was then determined by monitoring the integration of the peak for the amide proton resonance as a function of time.

Procedure for Monitoring the Rate of Ring-Opening Reaction of Monomer 1a. In a capped 4 mL glass vial prefilled with N_2, fresh catalyst **3** (10 μmol, 1 equiv) was dissolved in 100 μL of indicated solvent including chloroform, dichloromethane, dichloroethane, benzene, and toluene. Then 50 μL of amide **1a** (10 μmol, 1 equiv) was added, and the reaction mixture was heated at the selected temperature (20, 35, 55, and 85 °C) for 5 min. 1 μL of the reaction mixture was collected and analyzed by ESI-MS in direct injection positive mode with a final concentration of 50 μg/mL in methylene chloride. The ratio of the intensity of the protonated **1a** $[MH^+]$ ion at m/z 194.1 to the intensity of $H_2IMes{\cdot}H^+$ at m/z 307 was calculated to estimate the extent of reaction.[25]

DOI: 10.1021/acs.macromol.8b00562
Macromolecules 2018, 51, 3932−3940

General Procedure for AROMP Formation of Oligomers. Synthesis of AROMP oligomers was conducted under an N_2 atmosphere in a 4 mL glass vial in dried $CHCl_3$. 100 μL of fresh catalyst **3** (8.9 mg, 10 μmol, 1 equiv) solution was mixed with the indicated amount of monomer **1**. The mixture was heated at 85 °C for 5 min to initiate reaction in a sealed vial capped with a PTFE linear. After monomer **1** was completely reacted as judged by the disappearance of target m/z in the ESI-MS spectrum, the reaction temperature was then lowered to 45 °C and monomer **2** was added. The reaction was then heated and stirred at 45 °C for 15 min to ensure incorporation of **2**. The process was repeated until all desired monomers were incorporated. Ethyl vinyl ether (50 equiv) was added, and the reaction was stirred for another 10 min at 20 °C to quench the reaction. The solvent was evaporated, and the synthesized oligomers were purified by silica column chromatography with a step gradient (100% CH_2Cl_2 to remove contaminants, then 20:1/CH_2Cl_2:MeOH to elute oligomer). The theoretical number-average molecular weight M_n^{theor} was calculated from the monomer:catalyst feed ratio.

P1: *Poly[(**1a**-alt-**2**)$_1$-block-(**1b**-alt-**2**)$_1$]$_6$.* Amide monomer **1a** (1.9 mg, 10 μmol, 1 equiv) was dissolved in 20 μL of $CHCl_3$ and mixed with 100 μL of catalyst **3** (8.9 mg, 10 μmol, 1 equiv). The reaction was heated at 85 °C for 5 min in a capped vial. After complete initiation (solution color changed from light green to wine red), the reaction temperature was lowered to 45 °C and monomer **2** (1 μL, 10 μmol, 1 equiv) was added. The reaction solution was heated at 45 °C for another 15 min. Complete incorporation was judged by the disappearance of **1a** (m/z: $[M + H]^+$ 194.1). Then the reaction temperature was raised again to 85 °C, and amide monomer **1b** (2.23 mg, 10 μmol, 1 equiv) in 20 μL of $CHCl_3$ was added; the reaction mixture was heated at 85 °C for 5 min. Then at 45 °C, monomer **2** (1 μL, 10 μmol, 1 equiv) was added. The reaction was heated at 45 °C for another 15 min. ESI-MS confirmed complete conversion of **1b** (m/z: $[M + H]^+$ 224.1). The addition of monomers **1** and **2** was repeated for five more cycles to incorporate all desired monomers. An ESI-MS spectrum was acquired after each addition step, and the absence of target ion was judged to indicate successful incorporation of the monomer units. Ethyl vinyl ether (50 equiv) was added, and the reaction was stirred for 10 min at 20 °C to quench the reaction. Flash column chromatography of the crude product yielded poly[(**1a**-*alt*-**2**)-*block*-(**1b**-*alt*-**2**)]$_6$ (20 mg, 57% yield). ^{1}H NMR (700 MHz, CD_2Cl_2): δ 7.45−7.27 (m, 5H, Ph), 6.41 (m, 6H, CONH), 6.27 (t, J = 7.0 Hz, 6H, =CH), 6.13 (t, J = 7.0 Hz, 6H, =CH), 5.94 (m, 6H, CONH), 5.10 (m, 12H, =CH), 4.05 (m, 12H, CH_2), 3.76 (m, 18H, CH_3), 3.21 (m, 12H, CH_2), 2.58 (m, 15H), 2.39 (m, 10H), 2.13−2.04 (m, 89H), 1.61−1.38 (m, 146H), 0.95 (m, 18H). ^{13}C NMR (126 MHz, CD_2Cl_2): δ 170.6, 169.8, 141.8, 136.9, 136.2, 135.8, 134.5, 128.9, 128.3, 120.9, 43.5, 41.3, 33.0, 29.9, 28.4, 28.0, 26.9, 23.8, 23.0, 20.8, 14.0, 11.3. M_n^{theor} = 3.7 kDa. M_n^{GPC} = 2.7 kDa. M_w^{GPC} = 3.6 kDa. $Đ_M$ = 1.3.

P2: *Poly[(**1a**-alt-**2**)$_2$-block-(**1b**-alt-**2**)$_2$]$_3$.* Amide monomer **1a** (3.9 mg, 20 μmol, 2 equiv) was dissolved in 40 μL of $CHCl_3$ and mixed with 100 μL of fresh catalyst **3** (8.9 mg, 10 μmol, 1 equiv). The reaction was then heated at 85 °C for 5 min in a capped vial. The reaction was cooled to 45 °C after complete initiation of **1a**. Monomer **2** (2 μL, 20 μmol, 2 equiv) was then added, and the reaction was heated at 45 °C for another 20 min. A 1 μL aliquot of the reaction was collected by syringe for ESI-MS to determine if incorporation of **1a** was complete. The reaction temperature was raised to 85 °C, and amide monomer **1b** (4.5 mg, 20 μmol, 2 equiv) in 40 μL of $CHCl_3$ was added. The reaction was heated for 5 min at 85 °C. Then monomer **2** (2 μL, 20 μmol, 2 equiv) was added at 45 °C and heated for another 20 min. Completion of reaction was determined by the disappearance of protonated **1b** in the ESI-MS spectrum. The addition of monomer pairs was repeated two more times to incorporate all desired monomers. Ethyl vinyl ether (50 equiv) was then added, and the reaction was stirred for 10 min at 20 °C to quench the reaction. Flash column chromatography of the crude product yielded poly[(**1a**-*alt*-**2**)$_2$-*block*-(**1b**-*alt*-**2**)$_2$]$_3$ (22 mg, 61% yield). ^{1}H NMR (700 MHz, CD_2Cl_2): δ 7.45−7.27 (m, 5H, Ph), 6.40 (m, 6H, CONH), 6.27 (t, J = 7.0 Hz, 6H, =CH), 6.13 (t, J = 7.0 Hz, 6H, =CH), 5.92 (m, 6H, CONH), 5.09 (m, 12H, =CH), 4.05 (m, 12H, CH_2), 3.76 (m, 18H, CH_3), 3.22 (m, 12H, CH_2), 2.58 (m, 14H), 2.41 (m, 10H), 2.13−2.04 (m, 86H), 1.62−1.38 (m, 154H), 0.95 (m, 18H). ^{13}C NMR (126 MHz, CD_2Cl_2): δ 170.6, 169.8, 141.8, 136.9, 136.2, 135.7, 134.5, 128.9, 128.3, 120.9, 43.5, 41.3, 33.0, 29.9, 28.4, 28.0, 26.9, 25.1, 23.0, 20.8, 14.0, 11.3. M_n^{theor} = 3.7 kDa. M_n^{GPC} = 2.7 kDa. M_w^{GPC} = 3.6 kDa. $Đ_M$ = 1.3.

P3: *Poly[(**1a**-alt-**2**)$_3$-block-(**1b**-alt-**2**)$_3$]$_2$.* Amide monomer **1a** (5.8 mg, 30 μmol, 3 equiv) was dissolved in 60 μL of $CHCl_3$ and mixed with 100 μL of fresh catalyst **3** (8.9 mg, 10 μmol, 1 equiv). The reaction was then heated at 85 °C for 5 min in a capped vial. Then the reaction was cooled to 45 °C, and monomer **2** (3 μL, 30 μmol, 3 equiv) was added. The reaction was heated at 45 °C for another 20 min. The absence of target ion for protonated **1a** (m/z 194.1) in the ESI-MS spectrum indicated complete incorporation of **1a**. Amide monomer **1b** (6.7 mg, 30 μmol, 3 equiv) in 60 μL of $CHCl_3$ was then added at 85 °C, and the reaction was heated for 5 min. The reaction temperature was then lowered to 45 °C, and monomer **2** (3 μL, 30 μmol, 3 equiv) was added. The reaction mixture was heated at 45 °C for another 20 min. Completion of reaction was determined by the disappearance of protonated **1b** (m/z: $[M + H]^+$ 224.1) in the ESI-MS spectrum. The addition of monomer pairs was then repeated one more time to incorporate all desired monomers. To quench the reaction, ethyl vinyl ether (50 equiv) was then added in excess, and the reaction was stirred at 20 °C for 10 min. Flash column chromatography of the crude product yielded poly[(**1a**-*alt*-**2**)$_3$-*block*-(**1b**-*alt*-**2**)$_3$]$_2$ (23 mg, 65% yield). ^{1}H NMR (700 MHz, CD_2Cl_2): δ 7.45−7.27 (m, 5H, Ph), 6.40 (m, 6H, CONH), 6.27 (t, J = 7.0 Hz, 6H, =CH), 6.13 (t, J = 7.0 Hz, 6H, =CH), 5.92 (m, 6H, CONH), 5.09 (m, 12H, =CH), 4.05 (m, 12H, CH_2), 3.76 (m, 18H, CH_3), 3.22 (m, 12H, CH_2), 2.58 (m, 14H), 2.41 (m, 10H), 2.13−2.04 (m, 86H), 1.62−1.38 (m, 154H), 0.95 (m, 18H). ^{13}C NMR (126 MHz, CD_2Cl_2): δ 170.6, 169.8, 141.8, 136.9, 136.2, 135.7, 134.5, 128.9, 128.3, 120.8, 43.5, 41.3, 33.0, 29.9, 28.4, 28.0, 26.9, 23.8, 23.0, 20.8, 14.0, 11.3. M_n^{theor} = 3.7 kDa. M_n^{GPC} = 2.6 kDa. M_w^{GPC} = 3.5 kDa. $Đ_M$ = 1.3.

P4: *Poly[(**1a**-alt-**2**)$_4$-block-(**1b**-alt-**2**)$_4$]$_1$.* Amide monomer **1a** (7.7 mg, 40 μmol, 4 equiv) was dissolved in 80 μL of $CHCl_3$ and mixed with 100 μL of fresh catalyst **3** (8.9 mg, 10 μmol, 1 equiv). The reaction was then heated at 85 °C for 5 min in a capped vial. Monomer **2** (4 μL, 40 μmol, 4 equiv) was added into the reaction at 45 °C after completion of initiation. The reaction mixture was then heated at 45 °C for another 20 min. A 1 μL aliquot of the reaction was collected for ESI-MS, and no target ion for protonated **1a** (m/z: $[M + H]^+$ 194.1) was observed, indicating complete incorporation of **1a**. Amide monomer **1b** (8.9 mg, 40 μmol, 4 equiv) in 80 μL of $CHCl_3$ was then added at 85 °C, and the solution was heated again for 5 min. The reaction was then cooled to 45 °C. Monomer **2** (4 μL, 40 μmol, 4 equiv) was added and heated at 45 °C for another 20 min. Complete reaction was determined by the disappearance of protonated **1b** (m/z: $[M + H]^+$ 224.1) in the ESI-MS spectrum. Ethyl vinyl ether (50 equiv) was then added, and the reaction was stirred for 10 min at 20 °C to quench the reaction. Flash column chromatography of the crude product yielded poly[(**1a**-*alt*-**2**)$_4$-*block*-(**1b**-*alt*-**2**)$_4$]$_1$ (15 mg, 66% yield). ^{1}H NMR (700 MHz, CD_2Cl_2): δ 7.45−7.27 (m, 5H, Ph), 6.41 (m, 4H, CONH), 6.27 (t, J = 7.0 Hz, 4H, =CH), 6.13 (t, J = 7.0 Hz, 4H, =CH), 5.91 (m, 4H, CONH), 5.10 (m, 8H, =CH), 4.05 (m, 8H, CH_2), 3.76 (m, 12H, CH_3), 3.22 (m, 8H, CH_2), 2.58 (m, 8H), 2.40 (m, 8H), 2.13−2.04 (m, 54H), 1.62−1.38 (m, 100H), 0.95 (m, 12H). ^{13}C NMR (126 MHz, CD_2Cl_2): δ 170.6, 169.7, 141.8, 137.0, 136.3, 135.7, 133.8, 128.8, 128.3, 120.8, 43.5, 41.3, 33.1, 29.9, 28.4, 28.0, 26.9, 23.8, 23.0, 20.8, 14.0, 11.3. M_n^{theor} = 2.6 kDa. M_n^{GPC} = 2.1 kDa. M_w^{GPC} = 2.4 kDa. $Đ_M$ = 1.2.

P5: *Poly[(**1a**-alt-**2**)$_5$-block-(**1b**-alt-**2**)$_5$]$_1$.* Amide monomer **1a** (9.7 mg, 50 μmol, 5 equiv) was dissolved in 100 μL of chloroform and mixed with 100 μL of fresh catalyst **3** (8.9 mg, 10 μmol, 1 equiv). The reaction was heated at 85 °C for 5 min in a capped vial to obtain complete initiation and then cooled to 45 °C. Monomer **2** (5 μL, 50 μmol, 5 equiv) was then added, and the solution was heated at 45 °C for another 20 min. A 1 μL aliquot of the reaction was collected by syringe for ESI-MS, and no target ion for protonated **1a** (m/z: $[M + H]^+$ 194.1) was observed. Amide monomer **1b** (11.2 mg, 50 μmol, 5

DOI: 10.1021/acs.macromol.8b00562
Macromolecules 2018, 51, 3932−3940

equiv) in 100 μL of $CHCl_3$ was then added at 85 °C, and the reaction was heated again for 5 min. After that, the reaction temperature was lowered to 45 °C. Then monomer **2** (5 μL, 50 μmol, 5 equiv) was added, and the reaction was heated at 45 °C for another 20 min. Complete reaction was determined by the disappearance of protonated **1b** (*m*/*z*: $[M + H]^+$ 224.1) in the ESI-MS spectrum. Ethyl vinyl ether (50 equiv) was then added, and the reaction was stirred for 10 min at 20 °C to quench the reaction. Flash column chromatography of the crude product yielded poly[(**1a**-*alt*-**2**)$_5$-*block*-(**1b**-*alt*-**2**)$_5$]$_1$ (20 mg, 66% yield). ^{1}H NMR (700 MHz, CD_2Cl_2): δ 7.45−7.27 (m, 5H, Ph), 6.40 (m, 5H, CONH), 6.27 (t, *J* = 7.0 Hz, 5H, =CH), 6.13 (t, *J* = 7.0 Hz, 5H, =CH), 5.92 (m, 6H, CONH), 5.10 (m, 10H, =CH), 4.05 (m, 10H, CH_2), 3.76 (m, 15H, CH_3), 3.22 (m, 10H, CH_2), 2.58 (m, 10H), 2.41 (m, 10H), 2.16−2.04 (m, 74H), 1.69−1.38 (m, 106H), 0.95 (m, 15H). ^{13}C NMR (126 MHz, CD_2Cl_2): δ 170.6, 169.7, 141.9, 136.9, 136.2, 135.9, 134.5, 128.9, 128.3, 120.8, 43.5, 41.3, 33.2, 29.9, 28.4, 28.0, 26.9, 23.9, 23.0, 20.8, 13.7, 11.3. M_n^{theor} = 3.1 kDa. M_n^{GPC} = 2.8 kDa. M_w^{GPC} = 3.2 kDa. $Đ_M$ = 1.2.

***P6**: Poly[(**1a**-alt-**2**)$_6$-block-(**1b**-alt-**2**)$_6$]$_1$.* Amide monomer **1a** (11.6 mg, 60 μmol, 6 equiv) was dissolved in 100 μL of $CHCl_3$ and mixed with 100 μL of fresh catalyst **3** (8.9 mg, 10 μmol, 1 equiv). The reaction was then heated at 85 °C for 5 min. After complete initiation, the reaction was cooled to 45 °C and monomer **2** (6 μL, 60 μmol, 6 equiv) was added. The solution was heated at 45 °C for another 30 min. A 1 μL aliquot of the reaction was collected by syringe for ESI-MS, and no target ion for protonated **1a** (*m*/*z*: $[M + H]^+$ 194.1) was observed, indicating complete incorporation of **1a**. The reaction temperature was raised again to 85 °C, and amide monomer **1b** (13.4 mg, 60 μmol, 6 equiv) in 100 μL of $CHCl_3$ was added. The reaction mixture was heated again at 85 °C for 5 min. Then monomer **2** (6 μL, 60 μmol, 6 equiv) was added at 45 °C and heated for another 30 min. Complete reaction was determined by the disappearance of protonated **1b** (*m*/*z*: $[M + H]^+$ 224.1) in the ESI-MS spectrum. Ethyl vinyl ether (50 equiv) was then added, and the reaction was stirred for 10 min at 20 °C to quench the reaction. Flash column chromatography of the crude product yielded poly[(**1a**-*alt*-**2**)$_6$-*block*-(**1b**-*alt*-**2**)$_6$]$_1$ (24 mg, 68% yield). ^{1}H NMR (700 MHz, CD_2Cl_2): δ 7.45−7.27 (m, 5H, Ph), 6.40 (m, 6H, CONH), 6.27 (t, *J* = 7.0 Hz, 6H, =CH), 6.13 (t, *J* = 7.0 Hz, 6H, =CH), 5.92 (m, 6H, CONH), 5.09 (m, 12H, =CH), 4.05 (m, 12H, CH_2), 3.76 (m, 18H, CH_3), 3.22 (m, 12H, CH_2), 2.58 (m, 14H), 2.41 (m, 10H), 2.13−2.04 (m, 86H), 1.62−1.38 (m, 154H), 0.95 (m, 18H). ^{13}C NMR (126 MHz, CD_2Cl_2): δ 170.6, 169.7, 141.4, 136.9, 136.2, 135.7, 133.8, 128.9, 128.3, 120.4, 60.1, 43.5, 41.3, 33.1, 29.9, 28.4, 28.0, 26.9, 23.8, 23.0, 20.8, 14.0, 11.3. M_n^{theor} = 3.7 kDa. M_n^{GPC} = 2.8 kDa. M_w^{GPC} = 3.8 kDa. $Đ_M$ = 1.3.

***Pr**: Poly[(**1a**-alt-**2**)-ran-(**1b**-alt-**2**)]$_6$.* Amide monomer **1a** (11.6 mg, 60 μmol, 6 equiv) and amide monomer **1b** (13.4 mg, 60 μmol, 6 equiv) were dissolved in 100 μL of $CHCl_3$ and mixed with 100 μL of fresh catalyst **3** (8.9 mg, 10 μmol, 1 equiv). The reaction was then heated at 85 °C for 5 min in a capped vial. After complete initiation, the reaction temperature was lowered to 45 °C. Monomer **2** (20 μL, 180 μmol, 18 equiv) was added and heated at 45 °C for 120 min. A 1 μL aliquot of the reaction was collected by syringe for ESI-MS, and no target ion for protonated **1a** (*m*/*z*: $[M + H]^+$ 194.1) or **1b** (*m*/*z*: $[M + H]^+$ 224.1) was observed, indicating completed incorporation of all monomers. Ethyl vinyl ether (50 equiv) was then added, and the reaction was stirred for 10 min at 20 °C to quench the reaction. Flash column chromatography of the crude product yielded poly[(**1a**-*alt*-**2**)-*ran*-(**1b**-*alt*-**2**)]$_6$ (24 mg, 68% yield). ^{1}H NMR (700 MHz, CD_2Cl_2): δ 7.45−7.27 (m, 5H, Ph), 6.40 (m, 6H, CONH), 6.27 (t, *J* = 7.0 Hz, 6H, =CH), 6.13 (t, *J* = 7.0 Hz, 6H, =CH), 5.92 (m, 6H, CONH), 5.09 (m, 12H, =CH), 4.05 (m, 12H, CH_2), 3.76 (m, 18H, CH_3), 3.22 (m, 12H, CH_2), 2.58 (m, 14H), 2.41 (m, 10H), 2.13−2.04 (m, 86H), 1.62−1.38 (m, 154H), 0.95 (m, 18H). ^{13}C NMR (126 MHz, CD_2Cl_2): δ 170.6, 169.1, 141.7, 136.7, 136.1, 135.7, 134.5, 128.9, 128.3, 120.8, 60.2, 43.5, 41.3, 33.0, 29.9, 28.4, 28.0, 26.9, 23.8, 23.0, 20.8, 14.0, 11.3. M_n^{theor} = 3.7 kDa. M_n^{GPC} = 3.6 kDa. M_w^{GPC} = 4.3 kDa. $Đ_M$ = 1.2.

***H1**: Poly(**1a**-alt-**2**)$_{12}$.* Amide monomer **1a** (23.2 mg, 120 μmol, 12 equiv) was dissolved in 100 μL of $CHCl_3$ and mixed with 100 μL of fresh catalyst **3** (8.9 mg, 10 μmol, 1 equiv). The reaction was heated at 85 °C for 5 min in a capped vial. After initiation, the reaction was cooled to 45 °C. Monomer **2** (12 μL, 12 μmol, 12 equiv) was added, and the reaction was then heated at 45 °C for 60 min. Ethyl vinyl ether (50 equiv) was then added, and the reaction was stirred for 10 min at 20 °C to quench the reaction. Flash column chromatography of the crude product yielded poly(**1a**-*alt*-**2**)$_{12}$ (24 mg, 73% yield). ^{1}H NMR (700 MHz, CD_2Cl_2): δ 7.45−7.27 (m, 5H, Ph), 6.13 (m, 12H, =CH), 5.92 (m, 12H, CONH), 5.09 (m, 12H, =CH), 3.22 (m, 24H, CH_2), 2.58 (m, 12H), 2.41 (m, 12H), 2.13−2.04 (m, 108H), 1.62−1.38 (m, 158H), 0.95 (m, 36H). M_n^{theor} = 3.5 kDa. M_n^{GPC} = 3.6 kDa. M_w^{GPC} = 3.8 kDa. $Đ_M$ = 1.1.

***H2**: Poly(**1b**-alt-**2**)$_{12}$.* Amide monomer **1b** (26.8 mg, 120 μmol, 12 equiv) was dissolved in 100 μL of $CHCl_3$ and mixed with 100 μL of fresh catalyst **3** (8.9 mg, 10 μmol, 1 equiv). The reaction was then heated at 85 °C for 5 min in a capped vial. After complete initiation, monomer **2** (12 μL, 120 μmol, 12 equiv) was added at 45 °C, and the reaction was heated for 60 min. Ethyl vinyl ether (50 equiv) was then added, and the reaction was stirred for 10 min at 20 °C to quench the reaction. Flash column chromatography of the crude product yielded poly(**1b**-*alt*-**2**)$_{12}$ (24 mg, 72% yield). ^{1}H NMR (700 MHz, CD_2Cl_2): δ 7.45−7.27 (m, 5H, Ph), 6.37 (m, 12H, CONH), 6.27 (m, 12H, =CH), 5.10 (m, 12H, =CH), 4.04 (m, 24H, CH_2), 3.76 (m, 36H, CH_3), 2.58 (m, 12H), 2.41 (m, 12H), 2.13−2.04 (m, 100H), 1.62−1.38 (m, 156H). M_n^{theor} = 3.9 kDa. M_n^{GPC} = 3.6 kDa. M_w^{GPC} = 3.8 kDa. $Đ_M$ = 1.1.

Contact Angle Measurement. Oligomer thin films were cast on a single side polished, 500 μm thick, small piece (1 × 1 cm^2) of silicon wafer (P/B type with orientation of (100)). Fresh sample solution (1 wt % in $CHCl_3$) was filtered with a syringe filter (pore size 0.45 μm). Prior to spin-coating, the silicon wafer was cleaned and dried under vacuum for 16 h. The synthesized oligomers were spin-coated at 2000 rpm for 30 s and then 5000 rpm for 5 s. The cast thin films were dried under vacuum for 2 h. The contact angle of pure water was then measured with a DataPhysics OCA contact angle instrument (Brookhaven National Lab, Brookhaven, NY) and analyzed with SCA20 software. 3 μL of water was dispensed onto the surface with a flow rate of 1.13 μL/s. Data for thin films fabricated from five different batches of the same oligomer were acquired. For each batch, two thin films were fabricated and the static contact angle was measured. The average value of all ten measurements is reported.

RESULTS AND DISCUSSION

We undertook development of a platform for nontemplated synthesis of oligomers with precise side-chain sequences. We optimized conditions to obtain complete reaction of 1 equiv of bicyclo[4.2.0]oct-1(8)-ene-8-carboxamide monomer, **1**. Oligomers with well-defined microblocks of **1a**-*alt*-**2** and **1b**-*alt*-**2** were synthesized in cycles via sequential addition of defined equivalents of monomers **1** and **2**. Monomers **1a** and **1b** were selected for development to explore the effects of controlling hydrophilic and hydrophobic microblock size.

Selection of Rapidly Reacting AROMP Monomers. The biggest challenge for optimal sequence control is obtaining a high conversion rate. Monomer with one side chain must be quantitatively consumed before addition of the next aliquot of monomer. Therefore, the alternating copolymerization of five different monomer **1** units with monomer **2** was conducted to compare their relative rates of reaction (Figure 1).

All five monomers underwent fast initiation when treated with catalyst **3**, and efficient propagation was observed upon addition of monomer **2**, indicating robust AROMP reactivity, although monomer **1e** was noticeably slower than the other four monomers. Both monomers **1a** and **1b** reacted completely within 1 h. These monomers were selected for further reaction development because their polarities were sufficiently different that sequence effects on material properties could be tested.

DOI: 10.1021/acs.macromol.8b00562
Macromolecules 2018, 51, 3932−3940

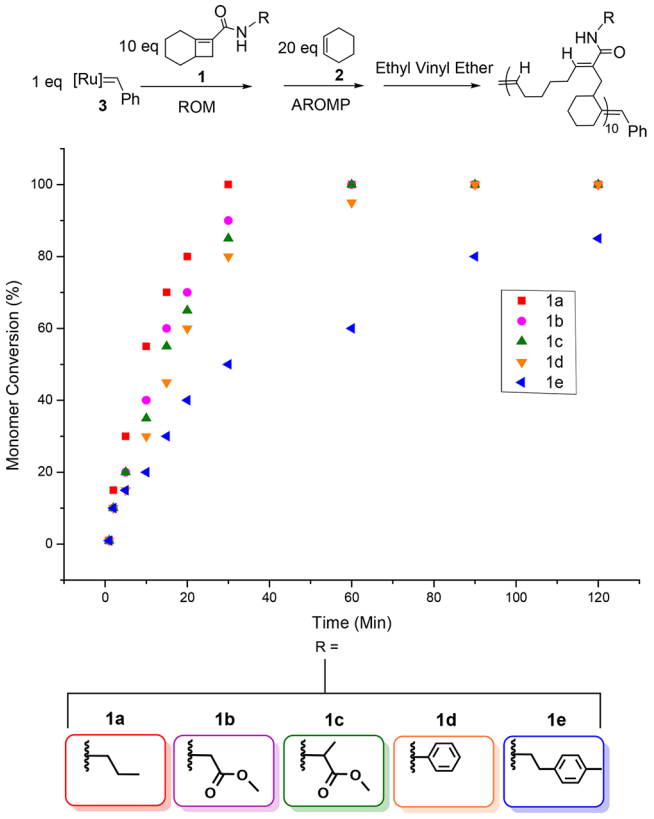

Figure 1. Monomers **1a** and **1b** AROMP most efficiently. Monomer **1**, monomer **2**, and catalyst **3** were mixed in a 10:20:1 ratio in $CDCl_3$, [**3**] = 0.01 M. Percent conversion was determined by ^1H NMR spectroscopy and integration of shifted side-chain peaks. Each experiment was performed at least twice, and data from a representative experiment are shown.

Increasing the Rate of Monomer Reaction. Although monomers **1a** and **1b** undergo rapid AROMP, to achieve stepwise addition of single monomers to a growing polymer chain, higher reaction rates were required than observed under the initial conditions used. We investigated different approaches to enhance monomer **1a** reactivity.

Previous studies have shown that adding diluted Lewis acid to a ROMP reaction stabilizes the 14 e^- metal complex intermediate and increases catalyst reactivity.[26] In our system, minimal improvement of catalyst reactivity was observed when diluted HCl was added to **1a** and **3**. We assume this is due to the fast and efficient dissociation of ligands from catalyst **3** in comparison to earlier catalysts. Therefore, ligand dissociation is not the rate-limiting step for monomer initiation.

The effect of solvent and temperature on the ring-opening reaction of monomer **1a** was investigated. To monitor reaction progress, ESI-MS spectra were measured by direct injection of reaction mixtures.[25,27,28] The ratio of the intensity of protonated **1a**·$\mathbf{H}^+$ ion at m/z 194.1 to the intensity of $H_2IMes{\cdot}H^+$ at m/z 307 was used to estimate the percent of ring-opening that had occurred.[25] The extent of reaction was determined after treatment of 1 equiv of monomer **1a** with 1 equiv of catalyst **3** for 5 min.

Regardless of solvent, ring-opening of **1a** initiated at 20 °C (Figure 2). However, the reaction did not proceed to more than 50−65% completion within 5 min at 20 °C. Monomer ion was still observed in the ESI-MS spectrum with an extended reaction time of 20 min.

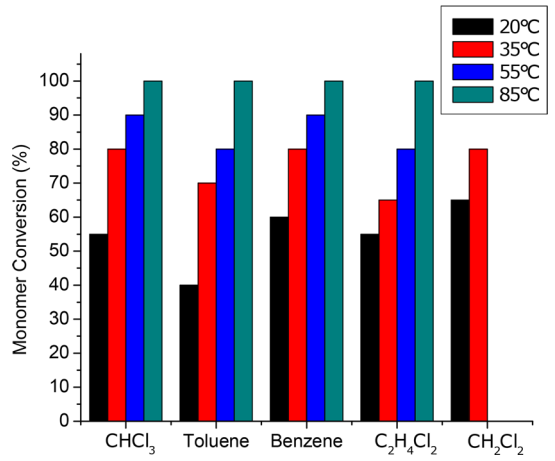

Figure 2. Rapid (5 min) ring-opening metathesis of **1a** requires high temperature. Monomer **1a** (1 equiv) was treated with catalyst **3** (1 equiv) for 5 min in the indicated solvent at four different temperatures. The extent of monomer ring-opening metathesis was estimated based on the disappearance of the **1a**·$\mathbf{H}^+$ ion at 194.1 in the ESI-MS spectrum. Each experiment was performed at least twice, and data from a representative experiment are shown.

Therefore, higher reaction temperatures were investigated. Rates of ring-opening increased from 20 to 85 °C. Importantly, 100% conversion of monomer **1a** was observed within 5 min at 85 °C in all solvents tested. Accordingly, 85 °C was selected as the optimal reaction temperature for stoichiometric monomer addition.

Although 100% conversion of **1a** was obtained at 85 °C, precipitation of oligomers was observed during AROMP, especially in benzene and toluene. In contrast, oligomers displayed excellent solubility in chloroform as well as high reactivity. Hence, chloroform was selected for further development of oligomer synthesis with specific sequences.

Oligomers with Controlled Sequences of Microblocks Can Be Synthesized by AROMP. Our first objective was to control the sequence of side chains on the polymer through stepwise chain growth AROMP. The initial catalyst concentration was 0.01 M, the same as used in the AROMP experiment of 10 identical monomer **1** units (Figure 1). The reaction mixture was analyzed by TLC and ESI-MS to assess whether complete incorporation of monomer occurred at each step.

After multiple steps of monomer addition, reduced reaction rates were observed. We hypothesized that the loss of reactivity was due to the dilution of active catalyst species. Therefore, we increased the starting catalyst concentration to 0.1 M. Meanwhile, we conducted the reaction in a larger scale to minimize the technical error from stoichiometric monomer addition. Complete reaction of monomer **1** was obtained, highlighting the critical importance of maintaining a high concentration of active catalytic species throughout the reaction process.

Herein, the experimental procedure was modified as well to further enhance the reactivity. The reaction solution was transferred to a new container with preweighed target monomer after complete incorporation of each monomer unit. The objective was to control the total volume of the reaction mixture while maintaining the catalyst/monomer ratio. With this synthetic protocol, near-quantitative monomer conversion was obtained with minimal precipitation for

DOI: 10.1021/acs.macromol.8b00562
Macromolecules 2018, 51, 3932−3940

oligomers with large microblocks like **P6** (Scheme 1). Unfortunately, in the case of **P1** and **P2**, where increased numbers of monomer addition steps were involved, lower overall conversion and stalled polymerization were observed as evidenced by ESI-MS even after prolonged polymerization times (>60 min).

We then modified the reaction temperature given that the reaction equilibrium was sensitive to temperature.[29] Initially, the polymerization was conducted at 85 °C in $CHCl_3$ for each single monomer addition step based on the results of the ROM experiment (Figure 2). The unfavorable decrease in entropy upon reaction progression is amplified at higher temperature in the case of ring-opening the unstrained cyclohexene **2**. Therefore, we redesigned the polymerization procedure to conduct the reaction at two different temperatures for monomers **1** and **2**. Incorporation of monomer **1** was conducted at 85 °C for a short period of time (5 min), with robust and complete incorporation confirmed by ESI-MS. The reaction mixture temperature was then lowered to 45 °C, after which monomer **2** was added, and the reaction was heated for an extended time at 45 °C (15−20 min). Addition of cyclohexene regenerates the catalytic species required for incorporation of the next carboxamide on the end of the growing chain. In contrast to the original procedure, where stalled propagation was observed in the later synthetic cycles, both **P1** and **P2** were synthesized with ease (Scheme 1).

The total reaction time for **P1**, for which the largest number of addition steps are involved, was shortened to 4 h from more than 24 h originally. The efficiency of the polymerization reaction was significantly increased, excluding the need for a reaction mixture transfer step between containers. Significantly, with this modified synthetic strategy, near-quantitative monomer conversion was obtained in each step so that the purification of intermediate was avoided. Building blocks of the synthetic oligomers were therefore controlled via this method of alternating two-stage reaction temperatures. The key point is the ease of control of introducing different side chain functionalities in a specified sequence while maintaining the backbone fidelity with quantitative monomer conversion.

Oligomers with Microblocks Have Identical Bulk Compositions. To analyze the effect of the size of the building block, oligomers **P1**, **P2**, **P3**, **P6**, and **Pr** were synthesized with the same total length to maintain identity of bulk composition. Shorter oligomers **P4** and **P5** were synthesized for use as comparison controls in select experiments. **H1** and **H2** are the homoside chain alternating oligomer controls that consist of purely $(\mathbf{1a}\text{-}alt\text{-}\mathbf{2})_{12}$ or $(\mathbf{1b}\text{-}alt\text{-}\mathbf{2})_{12}$, respectively. **P6** contains the largest microblocks, $(\mathbf{1a}\text{-}alt\text{-}\mathbf{2})_6$ and $(\mathbf{1b}\text{-}alt\text{-}\mathbf{2})_6$, which display hydrophilic and hydrophobic side chains, respectively, and only contains two segments. **P1** was synthesized with the smallest building block, $(\mathbf{1a}\text{-}alt\text{-}\mathbf{2})_1$ and $(\mathbf{1b}\text{-}alt\text{-}\mathbf{2})_1$. A random oligomer **Pr** was also synthesized with $(\mathbf{1a}\text{-}alt\text{-}\mathbf{2})_1$ and $(\mathbf{1b}\text{-}alt\text{-}\mathbf{2})_1$ incorporated in a single polymerization step. Given the similarity of monomer **1a** and **1b** reaction rates, the random polymer is close to statistical. Acquisition of MALDI-TOF spectra was undertaken to characterize oligomer sequences. However, oligomers were difficult to ionize and reproducible data was not collected. Herein, compositions of oligomers were confirmed by ^{1}H NMR and ^{13}C NMR spectroscopy.

The synthesized oligomers display identical NMR spectra (Figure 3a) with identical integrations indicating correct composition regardless of sequence. The olefin resonances in the ^{1}H NMR spectrum were sharp and could be assigned by comparison with spectra of **H1** and **H2** (Figure 3b). Furthermore, carbonyl and olefin resonances in the ^{13}C NMR spectra did not display any irregularities.

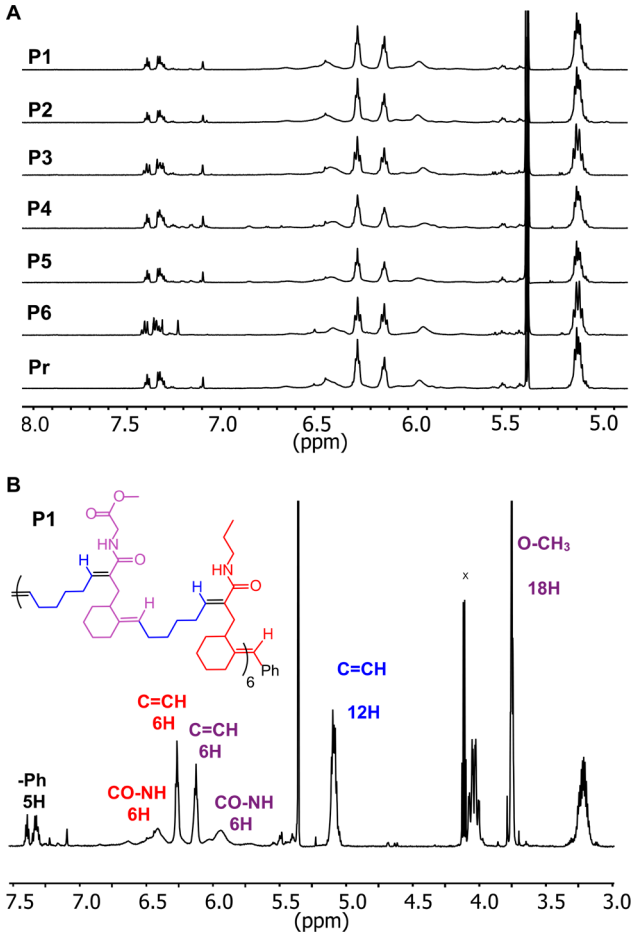

Figure 3. Composition of oligomers is independent of number of monomer addition cycles. ^{1}H NMR spectra (CD_2Cl_2) of oligomers **P1**−**P6** and **Pr** demonstrate the oligomers have the same bulk composition. (a) Stacked ^{1}H NMR spectra in the region of backbone olefin and terminal phenyl group. (b) Example integration of a oligomer spectrum. In **P1**, the ratio of **1a**:**1b**:**Ph** is 6:6:5 and is consistent with the feed ratio of **1a** and **1b** used to synthesize **P1**.

Multiblock oligomers were obtained as demonstrated by the experimental M_w and M_n (Table 1) measured by GPC (using UV absorption to detect). The experimental weights are in line with the theoretical molecular weights, and the oligomers have favorable dispersities ($Đ_m$ < 1.3). **Pr**, **H1**, and **H2** have relatively larger molecular weights and smaller $Đ_m$'s compared to the other copolymers (Figure 4). These characteristics are due to the higher monomer concentrations and shorter reaction times utilized for one-step polymerization step syntheses. The GPC traces (Figure S1) displayed monomodal weight distributions with small shoulders suggesting that linear structures were obtained with minimal, but observable, formation of macrocyclic byproducts.

Solution Structures Are Independent of Sequence. The solution behaviors of multiblock oligomers were investigated by measuring two-phase SAXS in an organic solvent. Oligomer samples were sealed in glass capillaries to prevent solvent evaporation and to ensure constant concentration. THF was selected as the solvent for SAXS measurements to maximize contrast between the solvent and polymer,

DOI: 10.1021/acs.macromol.8b00562
Macromolecules 2018, 51, 3932−3940

Table 1. Molecular Weights and Dispersities of Copolymers

polymer[a]	initiation ([3][b]:[1])	total time[c] (min)	M_n^{theor} [d] (kDa)	M_w^{GPC} [e] (kDa)	M_n^{GPC} [e] (kDa)	$Đ_M$
P1	1:1	240	3.7	3.6	2.7	1.3
P2	1:2	150	3.7	3.6	2.7	1.3
P3	1:3	80	3.7	3.5	2.6	1.3
P4	1:4	50	2.6	2.4	2.1	1.2
P5	1:5	50	3.1	3.2	2.8	1.2
P6	1:6	70	3.7	3.8	2.8	1.3
Pr	1:12	120	3.7	4.3	3.6	1.2
H1	1:12	65	3.5	3.8	3.6	1.1
H2	1:12	65	3.9	3.8	3.6	1.1

[a]All preparative polymerization experiments were performed five times. Representative molecular weight data are presented from a single polymerization. [b]The initial catalyst **3** concentration for all polymerization reaction was 0.1 M in $CHCl_3$. [c]Total reaction time is the time to complete all reaction steps. [d]Theoretical M_n is calculated from the monomer:catalyst feed ratio. [e]M_w and M_n were determined by GPC using UV detection and polystyrene standards.

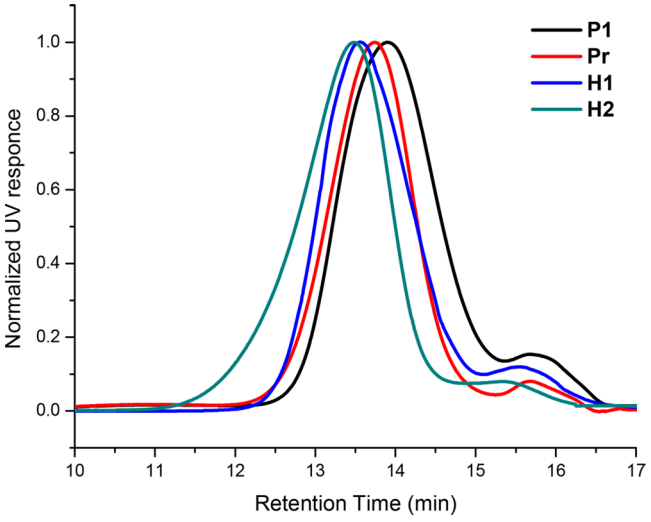

Figure 4. Overlay of GPC traces of representative oligomers. The oligomers were analyzed by GPC on a 0−500K MW mixed bed column with THF as the eluent at a flow rate of 0.7 mL/min at 30 °C. **P1**, the synthesis of which requires the most steps, and **Pr** have identical bulk compositions. **H1** and **H2** only contain a single monomer type. Full traces for all oligomers can be found in the Supporting Information (Figure S1).

despite moderate solubility of the polymer in THF. Poor signal intensity was recorded in all other solvents tested due to limited signal contrast between the solvent and the oligomer. The data collection time was 6 h to ensure moderate signal accumulation and to avoid the impact of any potential slow assembly or aggregation processes on the solution structure. All SAXS data were analyzed after subtraction of background THF signal.

To determine the best concentration for measurement and analysis, oligomer samples were prepared in THF at concentrations of 0.5−2.0 wt % (Figure S2A). The data at different concentrations have the same qualitative shape. Data for samples at 0.5 and 1.0 wt % do not show any peaks or evidence of aggregation. The lack of a correlation peak suggests that there are no strong interactions between oligomer chains in THF at these concentrations. A weak shoulder is observed for the data at 2.0 wt %, indicating that there may be some influence of interchain interactions on the solution structure at this concentration. We also do not observe an upturn in the intensity at low q for any of the concentrations. Normally, an upward signal intensity in the low q area is a sign of attractive interactions between polymer chains and formation of larger aggregates. There is an increase in intensity for the sample at 2.0 wt % as compared to the more dilute samples, but this is to be expected due to the higher concentration of oligomer.

Based on these results, oligomer samples were prepared in THF with a fixed concentration of 1.0 wt % for further SAXS measurement (Figure S2B). Preliminary analysis of oligomer (1% by weight) SAXS profiles in the mid-q range (0.025−0.15 $Å^{-1}$) yield a power-law dependence of the scattering intensity on q with exponent values near 1, suggesting a rodlike conformation of the oligomer in solution. The indicated rigid structure was unexpected considering the extended cyclohexene spacer, although it should be emphasized that this exponent was obtained over a limited range of q. No secondary interactions were observed based on the SAXS curve and basic fitting analysis. The lack of secondary structure was further confirmed by the absence of amide shifts in the IR spectra (Figure S3) for the same oligomer samples.

Surface Hydrophobicity Depends on Sequence. The influence of monomer distribution on thin film surface properties was investigated. To ensure accurate analysis,[30,31] sample solution concentrations (1 wt %), casting volumes (50 μL), and substrate scale (1 cm × 1 cm) were precisely controlled while spin-casting oligomer thin films. Moreover, water drop volume (3 μL) and delivery speed (1.13 μL/s) were precisely controlled to enhance measurement reproducibility. Each oligomer was synthesized five times, and two thin films were fabricated from each batch for use in surface property measurements. The fabricated thin films were examined by SEM and AFM, and the surface morphologies of all films were similarly smooth and uniform (Figure S4). In general, all oligomer thin films are relatively hydrophilic with an absolute contact angle value less than 90°.

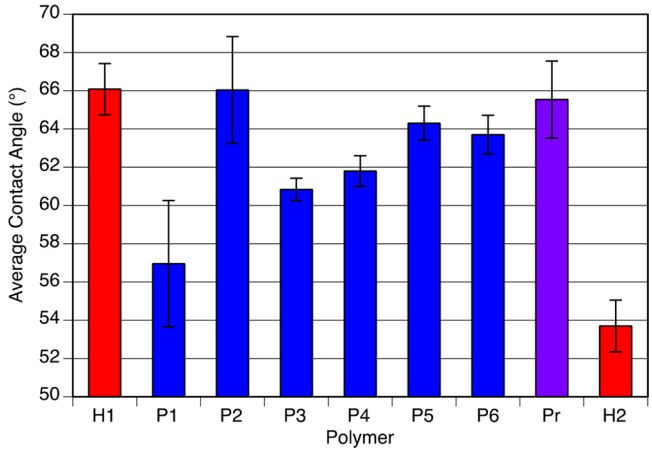

Figure 5. Surface hydrophobicity is dependent on microblock size, not bulk composition. Pure water droplet contact angles on oligomer thin films prepared by spin-coating were measured. Measurements were conducted with five different batches of each oligomer, and two measurements were taken for a single thin film for each synthetic batch of oligomer film. The error bars are the standard error of measurement based on a sample size of 10. Homocopolymers, **H1**: poly(**1a**-*alt*-**2**)$_{12}$; **H2**: poly(**1b**-*alt*-**2**)$_{12}$, are shown in red for reference. Random oligomer, **Pr**: poly[(**1a**-*alt*-**2**)-*ran*-(**1b**-*alt*-**2**)]$_6$, is shown in purple.

DOI: 10.1021/acs.macromol.8b00562
Macromolecules 2018, 51, 3932−3940

The contact angles on films of oligomers **H1** and **H2** were measured to establish the range of hydrophilicity attainable with the propyl and methyl glycine side chains, respectively. Oligomer **H1** displays only the hydrophobic propyl side chain. Oligomer **H2** displays a more hydrophilic methyl glycine side chain. The **H1** thin film displays the largest contact angle, and the **H2** thin film contact angle is 12° smaller, consistent with their side-chain compositions.

In contrast, the microblock oligomers displayed contact angle values in between those of the homocopolymers, and the angles varied with block size. In general, an increasingly larger contact angle was observed with increasing microblock size, despite the constant ratio of hydrophobic and hydrophilic side chains. This trend indicates that hydrophobicity depends on side-chain sequence and validated that our synthetic method generated oligomers with different sequences. Our data are consistent with earlier reports that the surface property of copolymer thin films can be influenced by the monomer composition as well as by the sequence or length of blocks.[32,33]

The contact angle of the surface can be predicted by summarizing the roughness or heterogeneity of the microphases:[34]

$$\cos\theta = \sum_{i=1}^{n} \gamma_i \cos\theta_i \quad (1)$$

where θ is the contact angle of the surface measured in bulk and γ_i is the factor for the fraction with "true" contact angle of θ_i. We postulate that as the microblock size increases, water droplet penetration is impeded due to phase separation, and hence a higher contact angle is observed. An exception was **P2**, for which a higher than expected hydrophobicity was observed (Figure 4). Varying block size can alter the orientation of side chains in addition to phase separation. We propose that the outer surface energy of the **P2** thin film is dominated by the orientation instead of phase separation, as is the case for other sequence-specific oligomers. Importantly, the distinct bulk behavior of the synthesized oligomer thin film demonstrates successful control of sequence and microblock size in AROMP oligomers.

CONCLUSION

A one-pot, nontemplated synthetic approach for the preparation of oligomers with well-controlled monomer sequences was developed. Rapid and near-quantitative monomer conversion was realized via facile, sequential addition of bicyclo[4.2.0]oct-1(8)-ene-8-carboxamide at 85 °C and cyclohexene at 45 °C. Strict cross-reactivity results in multiblock copolymers with side-chain sequence control.

Varying microblock size and monomer sequence resulted in identical solution behavior as measured by SAXS. Thin films were fabricated via spin-casting, and the surface energy of water droplets measured by contact angle revealed that increasing microblock size from one to six results in formation of an increasingly hydrophobic surface, despite the constant ratio of hydrophilic and hydrophobic side chains in the bulk material. An exception was observed if two carboxamides comprise the microblock. This sequence displays a relatively higher contact angle. The ability to control surface energy confirmed the successful synthesis of copolymers with controlled microblock sizes. Thus, AROMP provides entry into functional materials with a partially constrained all carbon backbone that can display well-controlled sequences of different functional groups.

ASSOCIATED CONTENT

Supporting Information

The Supporting Information is available free of charge on the ACS Publications website at DOI: 10.1021/acs.macromol.8b00562.

Additional experimental methods, data and spectra of compounds (PDF)

AUTHOR INFORMATION

Corresponding Author

*E-mail: Nicole.sampson@stonybrook.edu (N.S.S.).

ORCID

Guofang Li: 0000-0001-9298-1819

Nicole S. Sampson: 0000-0002-2835-7760

Notes

The authors declare no competing financial interest.

ACKNOWLEDGMENTS

We acknowledge funding from NSF CHE1609494 and NIH GM097971 (NSS). The SAXS and contact angle experiments used resources of the Center for Functional Nanomaterials, a U.S. Department of Energy Office of Science Facility at Brookhaven National Laboratory, under Contract DE-SC0012704. We thank Dr. D. Nykypanchuk for assistance with SAXS, Dr. G. Doerk for assistance with contact angle measurements, the AERTC facilities at Stony Brook for SEM and AFM, and Mr. F. Picart and Dr. J. Marecek for their assistance with NMR spectroscopy.

REFERENCES

(1) Jain, S.; Bates, F. S. On the Origins of Morphological Complexity in Block Copolymer Surfactants. *Science* **2003**, *300*, 460−464.

(2) Colquhoun, H.; Lutz, J.-F. Information-Containing Macromolecules. *Nat. Chem.* **2014**, *6*, 455.

(3) Lutz, J.-F.; Ouchi, M.; Liu, D. R.; Sawamoto, M. Sequence-Controlled Polymers. *Science* **2013**, *341*, 1238149.

(4) Solleder, S. C.; Zengel, D.; Wetzel, K. S.; Meier, M. A. A Scalable and High-Yield Strategy for the Synthesis of Sequence-Defined Macromolecules. *Angew. Chem., Int. Ed.* **2016**, *55*, 1204−1207.

(5) Porel, M.; Alabi, C. A. Sequence-Defined Polymers via Orthogonal Allyl Acrylamide Building Blocks. *J. Am. Chem. Soc.* **2014**, *136*, 13162−13165.

(6) Pfeifer, S.; Lutz, J.-F. A Facile Procedure for Controlling Monomer Sequence Distribution in Radical Chain Polymerizations. *J. Am. Chem. Soc.* **2007**, *129*, 9542−9543.

(7) Satoh, K.; Matsuda, M.; Nagai, K.; Kamigaito, M. AAB-Sequence Living Radical Chain Copolymerization of Naturally Occurring Limonene with Maleimide: An End-to-End Sequence-Regulated Copolymer. *J. Am. Chem. Soc.* **2010**, *132*, 10003−10005.

(8) Lutz, J.-F. Writing on Polymer Chains. *Acc. Chem. Res.* **2013**, *46*, 2696−2705.

(9) Malins, E. L.; Amabilino, S.; Yilmaz, G.; Isikgor, F. H.; Gridley, B. M.; Becer, C. R. Precise Insertion of Clickable Monomer Along Polymer Backbone by Dynamic Temperature Controlled Radical Polymerization. *Eur. Polym. J.* **2015**, *62*, 347−351.

(10) Zhang, J.; Matta, M. E.; Hillmyer, M. A. Synthesis of Sequence-Specific Vinyl Copolymers by Regioselective ROMP of Multiply Substituted Cyclooctenes. *ACS Macro Lett.* **2012**, *1*, 1383−1387.

(11) Weiss, R. M.; Short, A. L.; Meyer, T. Y. Sequence-Controlled Copolymers Prepared via Entropy-Driven Ring-Opening Metathesis Polymerization. *ACS Macro Lett.* **2015**, *4*, 1039−1043.

(12) Bornand, M.; Torker, S.; Chen, P. Mechanistically Designed Dual-Site Catalysts for the Alternating ROMP of Norbornene and Cyclooctene. *Organometallics* **2007**, *26*, 3585−3596.

DOI: 10.1021/acs.macromol.8b00562
Macromolecules 2018, 51, 3932−3940

(13) Vehlow, K.; Wang, D.; Buchmeiser, M. R.; Blechert, S. Alternating Copolymerizations Using a Grubbs-Type Initiator with an Unsymmetrical, Chiral N-Heterocyclic Carbene Ligand. *Angew. Chem., Int. Ed.* **2008**, *47*, 2615−2618.
(14) Choi, T. L.; Rutenberg, I. M.; Grubbs, R. H. Synthesis of A, B-Alternating Copolymers by Ring-Opening-Insertion-Metathesis Polymerization. *Angew. Chem., Int. Ed.* **2002**, *41*, 3839−3841.
(15) Jeong, H.; John, J. M.; Schrock, R. R.; Hoveyda, A. H. Synthesis of Alternating trans-AB Copolymers through Ring-Opening Metathesis Polymerization Initiated by Molybdenum Alkylidenes. *J. Am. Chem. Soc.* **2015**, *137*, 2239−2242.
(16) Elling, B. R.; Xia, Y. Living Alternating Ring-Opening Metathesis Polymerization Based on Single Monomer Additions. *J. Am. Chem. Soc.* **2015**, *137*, 9922−9926.
(17) Flook, M. M.; Ng, V. W.; Schrock, R. R. Synthesis of Cis, syndiotactic ROMP Polymers Containing Alternating Enantiomers. *J. Am. Chem. Soc.* **2011**, *133*, 1784−1786.
(18) Daeffler, C. S.; Grubbs, R. H. Catalyst-Dependent Routes to Ring-Opening Metathesis Alternating Copolymers of Substituted Oxanorbornenes and Cyclooctene. *Macromolecules* **2013**, *46*, 3288−3292.
(19) Song, A.; Parker, K. A.; Sampson, N. S. Synthesis of Copolymers by Alternating ROMP (AROMP). *J. Am. Chem. Soc.* **2009**, *131*, 3444−3445.
(20) Parker, K. A.; Sampson, N. S. Precision Synthesis of Alternating Copolymers via Ring-Opening Polymerization of 1-Substituted Cyclobutenes. *Acc. Chem. Res.* **2016**, *49*, 408−17.
(21) Tan, L.; Li, G.; Parker, K. A.; Sampson, N. S. Ru-Catalyzed Isomerization Provides Access to Alternating Copolymers via Ring-Opening Metathesis Polymerization. *Macromolecules* **2015**, *48*, 4793−4800.
(22) Tan, L.; Parker, K. A.; Sampson, N. S. A Bicyclo[4.2.0]octene-Derived Monomer Provides Completely Linear Alternating Copolymers via Alternating Ring-Opening Metathesis Polymerization (AROMP). *Macromolecules* **2014**, *47*, 6572−6579.
(23) Chen, L.; Li, L.; Sampson, N. S. Access to Bicyclo[4.2.0]octene Monomers To Explore the Scope of Alternating Ring-Opening Metathesis Polymerization. *J. Org. Chem.* **2018**, *83*, 2892.
(24) Love, J. A.; Morgan, J. P.; Trnka, T. M.; Grubbs, R. H. A Practical and Highly Active Ruthenium-based Catalyst that Effects the Cross Metathesis of Acrylonitrile. *Angew. Chem., Int. Ed.* **2002**, *41*, 4035−4037.
(25) Wang, H.-Y.; Yim, W.-L.; Guo, Y.-L.; Metzger, J. r. O. ESI-MS Studies and Calculations on Second-Generation Grubbs and Hoveyda−Grubbs Ruthenium Olefin Metathesis Catalysts. *Organometallics* **2012**, *31*, 1627−1634.
(26) Lynn, D. M.; Mohr, B.; Grubbs, R. H.; Henling, L. M.; Day, M. W. Water-Soluble Ruthenium Alkylidenes: Synthesis, Characterization, and Application to Olefin Metathesis in Protic Solvents. *J. Am. Chem. Soc.* **2000**, *122*, 6601−6609.
(27) Adlhart, C.; Hinderling, C.; Baumann, H.; Chen, P. Mechanistic Studies of Olefin Metathesis by Ruthenium Carbene Complexes using Electrospray Ionization Tandem Mass Spectrometry. *J. Am. Chem. Soc.* **2000**, *122*, 8204−8214.
(28) Hinderling, C.; Adlhart, C.; Chen, P. Olefin Metathesis of a Ruthenium Carbene Complex by Electrospray Ionization in the Gas Phase. *Angew. Chem., Int. Ed.* **1998**, *37*, 2685−2689.
(29) Patton, P. A.; Lillya, C. P.; McCarthy, T. J. Olefin Metathesis of Cyclohexene. *Macromolecules* **1986**, *19*, 1266−1268.
(30) Viville, P.; Lazzaroni, R.; Dubois, P.; Kotzev, A.; Geerts, Y.; Borcia, G.; Pireaux, J.-J. Impact of Silicone-Based Block Copolymer Surfactants on the Surface and Bulk Microscopic Organization of a Biodegradable Polymer, Poly (ε-caprolactone). *Biomacromolecules* **2003**, *4*, 696−703.
(31) Altay, E.; Yapaöz, M. A.; Keskin, B.; Yucesan, G.; Eren, T. Influence of Alkyl Chain Length on the Surface Activity of Antibacterial Polymers Derived from ROMP. *Colloids Surf., B* **2015**, *127*, 73−78.
(32) Li, L.; Chan, C.-M.; Weng, L. T. Effects of the Sequence Distribution of Poly (acrylonitrile− butadiene) Copolymers on the Surface Chemical Composition As Determined by XPS and Dynamic Contact Angle Measurements. *Macromolecules* **1997**, *30*, 3698−3700.
(33) Inoue, Y.; Watanabe, J.; Takai, M.; Yusa, S. i.; Ishihara, K. Synthesis of Sequence-Controlled Copolymers from Extremely Polar and Apolar Monomers by Living Radical Polymerization and Their Phase-Separated Structures. *J. Polym. Sci., Part A: Polym. Chem.* **2005**, *43*, 6073−6083.
(34) Murray, M.; Darvell, B. A Protocol for Contact Angle Measurement. *J. Phys. D: Appl. Phys.* **1990**, *23*, 1150−1155.

DOI: 10.1021/acs.macromol.8b00562
Macromolecules 2018, 51, 3932−3940